Hindawi Publishing Corporation
Mathematical Problems in Engineering
Volume 2012, Article ID 126521, 15 pages
doi:10.1155/2012/126521

Research Article

Evasive Maneuvers in Space Debris Environment and Technological Parameters

Antônio D. C. Jesus,[1] Rafael S. Ribeiro,[1] Alessandro Rossi,[2] and Ernesto Veira Neto[3]

[1] *DFIS-Feira de Santana, Departamento de Física, Universidade Estadual de Feira de Santana, 44.036-900 Feira de Santana, BA, Brazil*
[2] *ISTI-CNR and IFAC-CNR, Via Madonna del Piano 10, 50019 Sesto Fiorentino, Italy*
[3] *Departamento de Matemática, Faculdade de Engenharia de Guaratinguetá, Universidade Estadual Paulista, 12.516-410 Guaratinguetá, SP, Brazil*

Correspondence should be addressed to Ernesto Veira Neto, ernesto@feg.unesp.br

Received 1 June 2012; Revised 21 August 2012; Accepted 31 August 2012

Academic Editor: Xu Zhang

We present a study of collisional dynamics between space debris and an operational vehicle in LEO. We adopted an approach based on the relative dynamics between the objects on a collisional course and with a short warning time and established a semianalytical solution for the final trajectories of these objects. Our results show that there are angular ranges in 3D, in addition to the initial conditions, that favor the collisions. These results allowed the investigation of a range of technological parameters for the spacecraft (e.g., fuel reserve) that allow a safe evasive maneuver (e.g., time available for the maneuver). The numerical model was tested for different values of the impact velocity and relative distance between the approaching objects.

1. Introduction

On July 24, 1996, the first accidental collision between an operational satellite and a piece of debris was recorded: the French microsatellite *Cerise* was hit, at the relative velocity of 14.77 km/s, by a fragment of about 10 cm, coming from the explosion of an Ariane rocket upper stage that happened ten years before. As a matter of fact only a few debris were produced by this event due to the particular geometry of the collision. But this was a clear sign that collisions in space are indeed a real threat. In 1999 and 2000 there was a serious warning about a possible collision of the Iridium constellation [1, 2]. Then, 13 years later on February 10, 2009, 16 : 56 UTC, the much feared first accidental collision between two large spacecrafts took place. The satellite Iridium 33 collided against an old nonoperational Strela-2M, a Russian communication satellite (codenamed Cosmos 2251), launched on September

16, 1993. Both satellites were shattered, generating two large clouds of debris, including about 2000 trackable fragments larger than a few centimeters.

The Iridium event made clear that collision avoidance and space traffic management are going to be a fundamental part of the future space practices. All the unclassified spacecrafts currently in orbit are cataloged by the United States Strategic Command (USSTRATCOM) in the two-line Element (TLE) catalog. In this catalog about 16 000 objects are listed along with their current orbital parameters. The limiting size of the objects included in the catalog is about 5 to 10 cm below a few thousand km of altitude and about 0.5 to 1 m in higher orbits (up to geostationary). Only about 6% of the objects in the TLE catalog are operative satellites. Starting from the tracking data acquired by the SSN, the US Joint Space Operations Center (JspOC) is currently providing satellite operators with information on dangerous close approaches involving selected spacecraft. On the basis of this information the operators can now decide to perform avoidance maneuvers for their own satellites.

This practice will become more and more important in the future as all the long-term evolution models have shown that there is a growing risk of collision in Earth orbit for the coming years [3]. Moreover, collision avoidance, together with active debris removal, is apparently a mandatory mitigation measure to prevent the onset of a collisional cascading in the most crowded zones of LEO [4].

In this paper the possibility to perform a fast avoidance maneuver for a spacecraft on a collision course with a space debris is explored.

2. The Mathematical Model

In this work we use a reference system centered on the satellite, as shown in Figure 1. This reference frame is fixed in the satellite body with the x-direction pointed in direction opposed to Earth perpendicular to the satellite orbit, the y-direction is in the direction of satellite fly on the orbital plane, and the z-direction is normal to the satellite orbit. We based the mathematical model on Hill's equations [5, 6]. These equations describe the relative motion between two orbiting bodies, the active spacecraft and the space debris in our case. For the sake of simplicity the satellite orbit around the Earth is assumed to be circular (a reasonable assumption when dealing with LEO satellites whose orbits are almost circular). The angular velocity is therefore constant,

$$\vec{\omega} = \omega \hat{z}. \tag{2.1}$$

In the dynamical model for the orbital motion of the two objects, both gravitational and nongravitational forces are considered. The Cartesian components of the acceleration can be found by developing in the Taylor series the ratio $|\vec{r}|/|\vec{R}| \ll 1$ of the relative distance between the spacecraft and the debris, $\vec{r}$, and the distance of the spacecraft, $\vec{R}$, from the center of the Earth. The equations are

$$\begin{aligned} \ddot{x} - 2\omega\dot{y} + 3\omega^2 x &= f_x, \\ \ddot{y} + 2\omega\dot{x} &= f_y, \\ \ddot{z} + 3\omega^2 z &= f_z. \end{aligned} \tag{2.2}$$

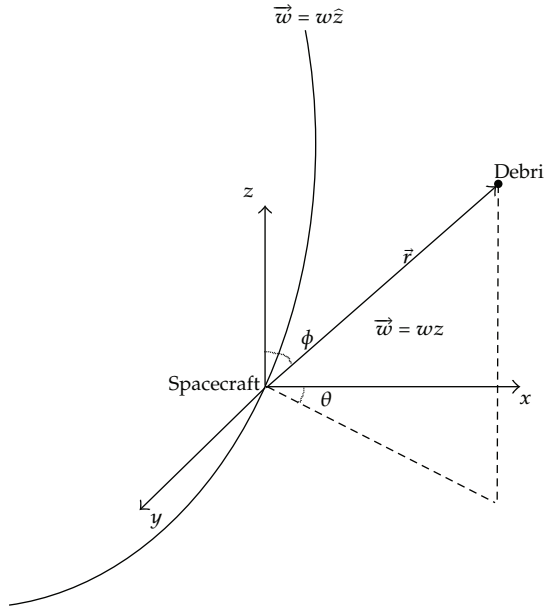

Figure 1: Orbital configuration and reference systems of the spacecraft and the approaching space debris around the Earth.

The homogeneous form is obtained when $f_x = f_y = f_z = 0$ which are called Clohessy-Wiltshire equations.

3. Avoidance Maneuvers Strategy

Equations (2.2) will be used to study evasive maneuvers in case of a possible collision detected *with a very short warning time*. The avoidance strategy is based on the following steps.

(1) First the solution of the homogeneous Clohessy-Wiltshire equations are found

$$x(t) = \frac{\dot{x}_0}{\omega}\sin\omega t - \left(\frac{2\dot{y}_0}{\omega} + 3x_0\right)\cos\omega t + \left(\frac{2\dot{y}_0}{\omega} + 4x_0\right),$$

$$y(t) = \frac{2\dot{x}_0}{\omega}\cos\omega t - \left(\frac{4\dot{y}_0}{\omega} + 6x_0\right)\sin\omega t + \left(y_0 - \frac{2\dot{x}_0}{\omega}\right) - (3y_0 + 6\omega x_0)t, \tag{3.1}$$

$$z(t) = z_0\cos\omega t + \frac{\dot{z}_0}{\omega}\sin\omega t.$$

(2) Then the equations of the Cartesian components of the initial relative velocity $(\dot{x}_0, \dot{y}_0, \dot{z}_0)$ between the two objects are found in terms of the Cartesian components

of the relative initial position (x_0, y_0, z_0). Let us call this solutions "collision course initial conditions" (CCIC):

$$x(t) = 0, y(t) = 0, z(t) = 0 \Longrightarrow r(t) = 0,$$

$$\begin{aligned} \dot{y}_0 &= \frac{\left[6x_0(\omega t \sin \omega t) - y_0\right]\omega \sin \omega t - 2\omega x_0(4 - 3\cos \omega t)(1 - \cos \omega t)}{(4 \sin \omega t - 3\omega t) \sin \omega t - 4(1 - \cos \omega t)^2}, \\ \dot{x}_0 &= -\frac{\omega x_0(4 - 3\cos \omega t) + 2(1 - \cos \omega t)\dot{y}_0}{\sin \omega t}, \\ \dot{z}_0 &= -\frac{\omega z_0 \cos \omega t}{\sin \omega t}. \end{aligned} \tag{3.2}$$

(3) With the CCIC we fix the time and initial distance between the two objects. This can be done in terms of the specific values of the initial relative velocities. The fixed time is called "collision time."

To perform the avoidance maneuvers simulations, values of the initial velocity compatible with the space debris velocities were selected. With the above equations many sets of initial conditions (position and velocity) and collision times can be found, for different ranges of space debris velocities. One of the CCIC and the related collision time were selected as the "nominal solution" to simulate evasive propulsion maneuvers. The choice of the nominal solution is not completely arbitrary, but rather a solution that better characterizes the real collisional conditions of space debris. We chose a solution where the relative velocity between the objects is approximately 8.0 km/s with nonplanar approach (i.e., both spherical angles, (θ, ϕ), are different from zero, see Figure 1). The average relative velocity of impact in LEO is approximately 10.0 km/s. This speed was found only for short collision times and it has a difficult implementation for evasive maneuvers. However, in this same region and with speeds of 8.0 km/s, spacecraft on a collision course with a debris has enough time to implement evasive maneuvers.

The collision time was set about 45 minutes, that is, we are considering very short warning time. This limit situation could be applied, for example, to a future situation on a spacecraft with active scanning radars on board or satellites in hostile environment. The choice of 45 minutes is not arbitrary, since for evasive maneuvers typically, on average, more than 20 minutes are required for internal calculation (on an on-board computer) for a new orbit of the vehicle in a collision course and its implementation.

To perform evasive maneuvers we exploited the solution of the nonhomogeneous equations describing the relative propelled motion (2.2). For this purpose we consider an exponential variation of the fuel mass as a function of time. This choice is motivated by the fact that we know that mass engines require high expenditure of energy per second, producing such high thrust. In this sense, engines more efficient with respect to the energy would be those which produce low thrust forces. The exponential model of the mass is more appropriate for this case.

The propulsion force depends on the following relations:

$$\begin{aligned} M(t) &= m_0 + m(t) \qquad M_0 \equiv \chi m_0, \\ M(t) &= m_0\left(\chi + e^{-\gamma t}\right), \quad \gamma > 0 \end{aligned} \tag{3.3}$$

and is given by

$$\vec{f} = \begin{cases} -v_{ex}\dfrac{d}{dt}\ln(M(t)), \\ -v_{ey}\dfrac{d}{dt}\ln(M(t)), \\ -v_{ez}\dfrac{d}{dt}\ln(M(t)). \end{cases} \tag{3.4}$$

With the non-homogeneous equations we performed numerical simulations of the relative coordinates and velocities during the collision time interval (found with the homogeneous solution without propulsion). With this procedure it is possible to verify if the selected collision time is enough to perform the evasive maneuver. If the time interval is long enough we find the physical (namely, the initial conditions) and the technological (propulsion system) characteristics allowing the avoidance maneuver.

The solution of the non-homogeneous equations is:

$$\begin{aligned} x(t) &= 2A\sin\omega t - 2B\cos\omega t + Et + \sum_{n=1}^{\infty} F_n e^{-n\gamma t} + G, \\ y(t) &= A\cos\omega t + B\sin\omega t + \sum_{n=1}^{\infty} C_n e^{-n\gamma t} + D, \\ z(t) &= H\cos\omega t + I\sin\omega t - \sum_{n=1}^{\infty} J_n e^{-n\gamma t}. \end{aligned} \tag{3.5}$$

The identified technological parameters are the gas exhaust velocity (v_{ex}, v_{ey}, v_{ez}), the power factor of the engine $(\gamma > 0)$, and the mass factor χ, that is, the mass ratio between the spacecraft mass (M_0) and the initial propellant mass (m_0).

The coefficients of the Cartesian coordinates and solution of the non-homogeneous equations are constant, given by

$$\begin{aligned} A &= \frac{2\dot{x}_0}{\omega} - 3y_0 + \frac{2v_{ex}}{\omega}\ln\left(\frac{\chi+1}{\chi}\right) - \sum_{n=1}^{\infty}\frac{(-1)^{n+1}}{n\chi^n}\left(\frac{2v_{ex}}{\omega} + \frac{n\gamma v_{ey}}{\omega^2}\right)\frac{1}{1+(n\gamma/\omega)^2}, \\ B &= \frac{\dot{y}_0}{\omega} + \frac{v_{ey}}{\omega}\ln\left(\frac{\chi+1}{\chi}\right) + \sum_{n=1}^{\infty}\frac{(-1)^{n+1}}{n\chi^n}\left(\frac{v_{ey}}{\omega} + \frac{2n\gamma v_{ex}}{\omega^2}\right)\frac{1}{1+(n\gamma/\omega)^2}, \\ E &= 6\omega y_0 - 3\dot{x}_0 - 3v_{ex}\ln\left(\frac{\chi+1}{\chi}\right), \end{aligned}$$

$$
\begin{aligned}
F_n &= \frac{(-1)^{n+1}}{n\chi^n}\left(\frac{2v_{ey}}{\omega}+\frac{4v_{ex}}{n\gamma}\right)\frac{1}{1+\left(n\gamma/\omega\right)^2}-\frac{v_{ex}}{n\gamma},\\
G &= \frac{2\dot{y}_0}{\omega}+x_0+\frac{2v_{ey}}{\omega}\ln\left(\frac{\chi+1}{\chi}\right)-\sum_{n=1}^{\infty}\frac{(-1)^{n+1}}{n^2\chi^n}\cdot\frac{3v_{ex}}{\omega},\\
C_n &= \frac{(-1)^{n+1}}{n\chi^n}\left(v_{ex}+\frac{n\gamma v_{ey}}{\omega^2}\right)\frac{1}{1+\left(n\gamma/\omega\right)^2},\\
D &= 4y_0-\frac{2\dot{x}_0}{\omega}-\frac{2v_{ex}}{\omega}\ln\left(\frac{\chi+1}{\chi}\right),\\
H &= z_0+\sum_{n=1}^{\infty}\frac{(-1)^{n+1}v_{ez}\gamma}{\chi^n\omega^2}\frac{1}{1+\left(n\gamma/\omega\right)^2},\\
I &= \frac{\dot{z}_0}{\omega}-\frac{v_{ez}}{\omega}\ln\left(\frac{\chi+1}{\chi}\right)+\sum_{n=1}^{\infty}\frac{(-1)^{n+1}}{n^2\chi^n\omega}v_{ez}\frac{1}{1+\left(n\gamma/\omega\right)^2},\\
J_n &= \frac{(-1)^{n+1}}{n\chi^n\omega}v_{ez}\frac{1}{1+\left(n\gamma/\omega\right)^2}.
\end{aligned}
\tag{3.6}
$$

The non-homogeneous solution on this dynamic, (3.5), has coefficients that depend on the technological parameters, as shown in (3.6). This means that evasive maneuvers can be controlled through the implementation of parameters that are defined by the available technology applied.

The mathematical relation between the mass factor and the power, for typical space flight situations, is as the following:

$$\chi = \frac{1-e^{-\gamma t}}{e^N-1}e^N, \tag{3.7}$$

$$N = \frac{\Delta V}{V_e}, \tag{3.8}$$

where ΔV is the velocity increment during the propulsion phase and V_e is the magnitude of the gas ejection velocity. N is therefore the consumption rate of the propellant for unit of escape velocity. For small orbit correction maneuvers N is typically lower than 1.

We simulate different evasive maneuvers, taking into account different space debris and space vehicles dimensions, the known collision time, and the final relative position of the two objects in space. Considering the space debris (r_d) and the space vehicle (r_v) as spherical objects, the collisions are analyzed based on the relations between their diameters. Note that varying the selected diameters we can also account for uncertainties in the orbit determination, that is, we can somehow account for the known covariance ellipsoid of the

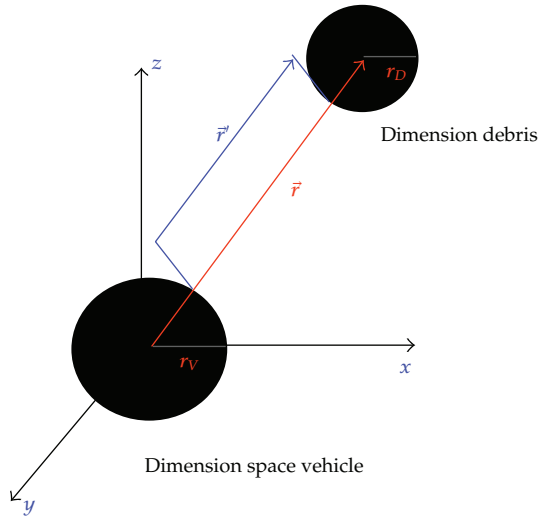

Figure 2: Collisional configuration of the "spherical" objects.

two objects (Figure 2). For the condition of minimal distance for the collision avoidance, the radii of the objects have to satisfy the following simple condition:

$$r' \geq 0 \Longrightarrow |\vec{r}| \geq D, \tag{3.9}$$

where

$$\begin{aligned} |\vec{r}| &= r' + r_d + r_v, \\ D &= r_d + r_v, \\ |\vec{r}| &= r' + D. \end{aligned} \tag{3.10}$$

Following the procedure outlined in this section we can find the allowed avoidance maneuvers on the basis of the identified parameters.

4. Results

In this section we will show the results of the numerical simulations of the parametric analysis of the avoidance maneuvers.

4.1. Collisional Configurations

Our analysis of the results depends on our set of initial conditions elements for some time interval. There is an infinity number of possible collisions and the problem changes quantitatively with the time interval. Then, we will use the technological limitations to restrict the time interval and analyze the collision only to a limited set of initial conditions.

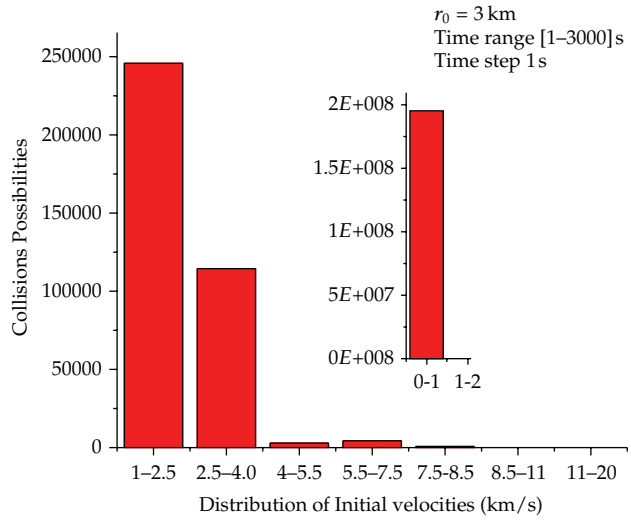

Figure 3: Collisions possibilities versus initial velocities distribution, $r = 3$ km.

The results of numerical simulation of the homogeneous solution equations on the relative dynamics allowed us to catalog the initial conditions favorable to collisions between space objects. This set of initial conditions was identified as the configurations that the collisional system (spacecraft debris) can take. That is, they are the states that the system can take on a collision course for relative distances between 3 and 500 km. The number of states are called "collision possibilities". In Figures 3–5 we show the distribution of the number of the collisional configurations (collision possibilities) relative to our set of initial condition and time interval of 0 s to 3 000 s, and a time step of 1 s, which we found considering the situation where the spacecraft is at the center of the reference system and the debris are initially on a sphere of radius variable from 3 to 500 km and is approaching the spacecraft with a velocity that can vary between 0 and 20 km/s. The limits above were conceived due to the technological feasibility and the precisions required for space missions.

These Figures give us an idea of the huge number of theoretical collisional configurations which we are dealing with in such a short-time interval.

Figures 4 and 5 show the upper end of the velocity distribution considered in the simulations. Figure 3 shows that the number of collisions is actually three orders of magnitude higher if low velocity (around 1 km/s) was considered.

It turns out that the vast majority of the collisions happen for very small values of the initial relative velocity and for very small initial distance between the objects. Nonetheless, from Figures 4 and 5, it can be also shown how larger values for the initial relative velocity and larger values for the initial separation and a significant number of collision possibilities could occur.

It is clear that large initial distances require large initial relative velocities to lead to a collision within the short-time span investigated while, for small initial distances, very small encounter velocities allow many collision configurations. Restricting the investigated time interval to a more reasonable reaction time, that is, from 1200 to 3000 seconds (e.g., see Figure 5), it can be shown that the general qualitative behavior is similar to the one observed for the whole-time interval.

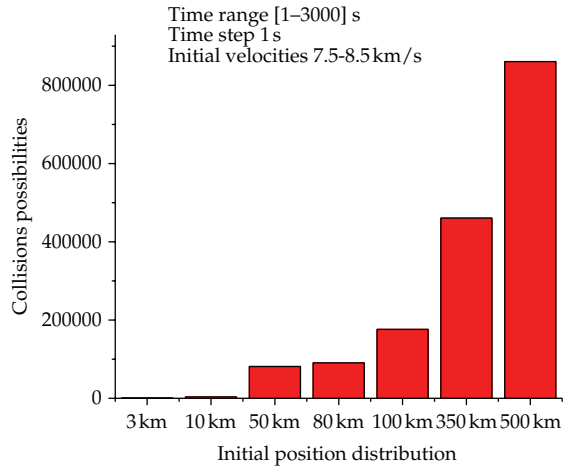

Figure 4: Collisions possibilities versus initial position distribution, v_0 = 7.5–8.5 km/s, time range: 1–3000 s.

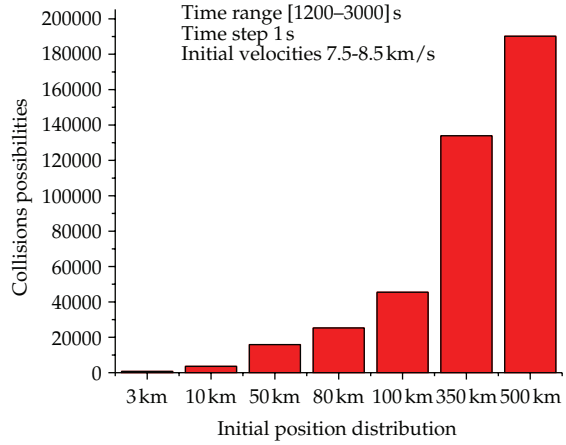

Figure 5: Collisions possibilities versus initial position distribution, v_0 = 7.5–8.5 km/s, time range: 1200–3000 s.

4.2. Dynamics of the Avoidance Maneuvers

In this section we outline the results of our simulations for avoidance maneuvers dynamics, based on parameters derived in the previous section.

Figure 6 shows the relation between the mass and power factors, as a function of N. Small values of N are preferred since they imply lower propellant consumption. The figure shows that small values of N still allow the choice of several different mass and power factors (i.e., different kind of engines) to perform the avoidance maneuver. Note that, from (3.8), the fuel consumption is related to the gas exhaust velocity. The power factor γ gives a measure of how fast the propellant is used by a given engine. Different values are listed and investigated since it is not easy to find in the open literature typical values for this technological parameter. The graphic confirms that for high power factor and low quantities of fuel the evasive maneuver will be possible to exhaust high speeds (small values of N).

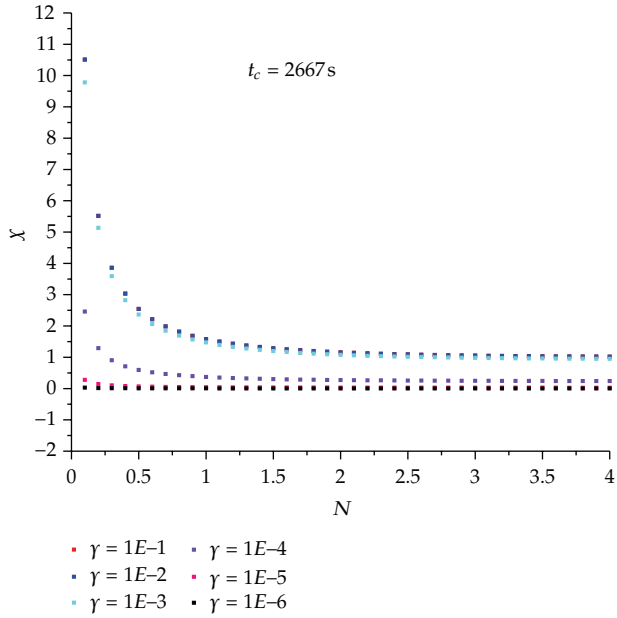

Figure 6: Relation between the mass and power factors, as a function of N for time collision 2667 s.

Maintaining the high exhaust velocity, the operation to lower power (due to technological limit) may be performed with less fuel (large values of χ).

In the following simulations the nominal solution chosen is initial relative distance r_0 = 3 km, angular coordinates out-plane $\phi = 68°$ and in-plane $\theta = 57°$, collision time = 2667 s, gas exhaust velocity = 2.5 km/s, initial relative velocity ~7.8 km/s, mass factor = 10, and power factor = 10^{-6}. The choice of the mass and power factors was done by using the values of N from (3.7) and (3.8). Of course the proper values are those that allow evasive maneuvers with ΔV values lower than the escape velocity, v_e, considering the limited amount of fuel on board for a typical spacecraft. Figure 7 shows the values of the two objects relative distance, as a function of time. The red line is the homogeneous nominal solution, that is, the no-propulsion case leading to a collision in 2667 s. The other lines refer to different power factors γ, for gas exhaust velocity of 2.5 km/s. We observed that as the values of γ grow, the corresponding curve moves away from the homogeneous line, featuring collisions with objects of larger sizes. This means it is possible to avoid collisions with even smaller objects with this value for this parameter.

Knowing the dimension of the objects (or better the dimension of the uncertainty envelope around each object) it is easy to determine if the avoidance maneuver is enough to avoid the collision. In particular, from Figure 7 it can be noticed how, for very short times, the propelled trajectories do not deviate significantly from the collision course. With growing time, the propelled trajectories separate from the nominal one, up to about 1000 km in the highest line. In all the propelled cases the collision is easily avoided by hundreds of km. Therefore we performed a set of simulation lowering significantly the power factor. Further lowering of γ the maneuver might not be effective to prevent the collision, taking into account the uncertainties involved in the process. Therefore, fixing the value of $\gamma = 10^{-6}$, Figure 8 shows the relative position as a function of time for different values of the ejection velocity, from 1.0 to 2.5 km/s.

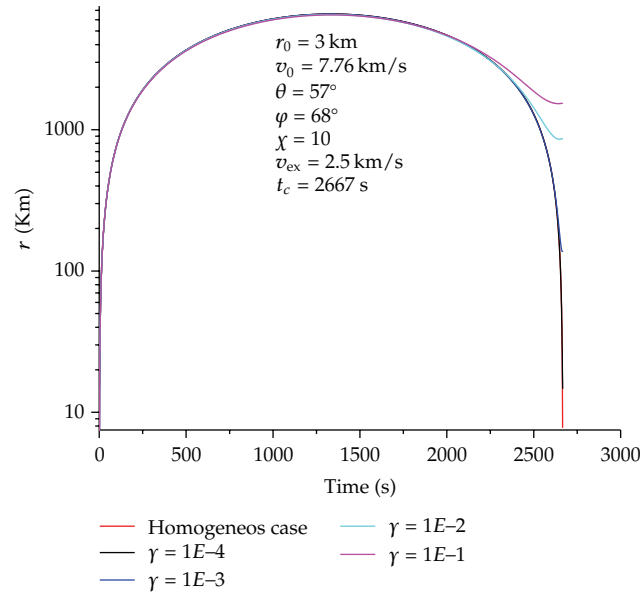

Figure 7: Relative position of the two objects as a function of time for different power factors.

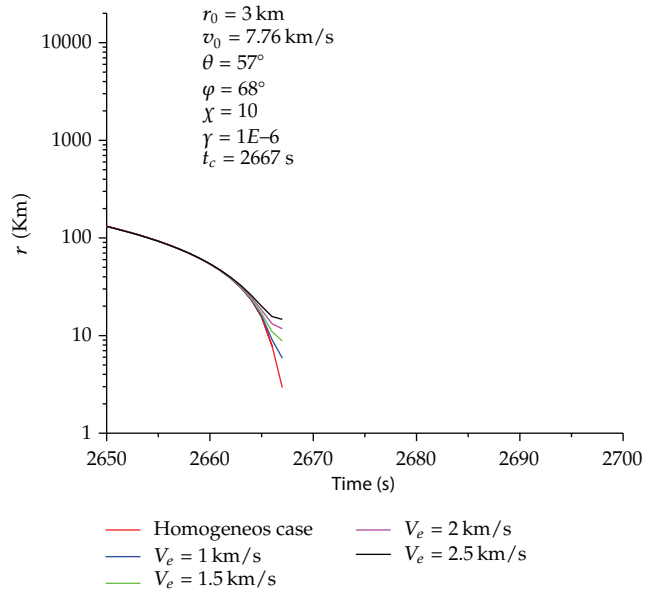

Figure 8: Relative position of the two objects as a function of time for different ejection velocity.

For all the chosen values of v_e the maneuver is enough to avoid the nominal collision (homogeneous case), even if, for the lowest values of v_e, the final miss distance is such that the possibility of a collision cannot be completely ruled out for large position uncertainty.

Figure 9 shows how the possibility to avoid a collision is related to the amount of fuel on board (χ) and to v_e. With large amount of fuel available (small χ) powerful maneuvers

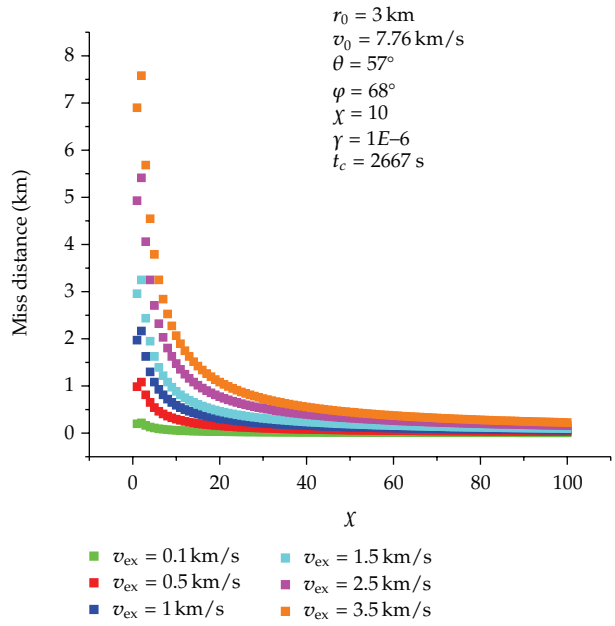

Figure 9: Relative final position between the two objects as a function of the mass factor for different gas exhaust velocities.

can be performed leading to large final separations. The situation reverses when we go to large values of χ. In this situation, it is not possible to implement an evasive maneuver in curse with large objects, even with high exhaust velocities. For this condition it will be only possible to implement evasive maneuvers with objects up to a few hundred meters.

Tables 1–3 give a numerical summary of some results described in this paper. In Table 1 the attainable miss distances after a maneuver as a function of mass factor and exhaust velocity are given. Table 2 shows the same miss distance as a function of the power factor and exhaust velocity. Table 3 gives the miss distance that can be reached starting from different initial distances (r_0) and initial relative velocities (v_0). For a very small initial separations it is clearly necessary to have considerable exhaust velocities, whereas for significant initial distance easier maneuvers can be performed. The sum of the radii of collisional objects (vehicle and debris) has maximum value represented by the miss distance. The effect of v_e is the removal of objects to maneuver with practically the same time of collision. When the initial relative position increases, the phenomenon is repeated with little variation in the time of collision due to the effect on the initial velocity.

5. Discussion and Conclusions

In this work we investigated the possibility to perform evasive maneuvers for a spacecraft in an extreme situation, such as a collisional course to a spatial debris and with very short time to reaction.

Our results highlighted the values of realistic technological parameters of a typical spacecraft for which an evasive maneuver can be performed for many different initial configurations. The technological parameters investigated include the engine power, the

Table 1: Miss distances after a maneuver as a function of mass factor and exhaust velocity.

χ	$v_e = 0.1\,\mathrm{km/s}$	$v_e = 0.5\,\mathrm{km/s}$	$v_e = 1.0\,\mathrm{km/s}$	$v_e = 1.5\,\mathrm{km/s}$	$v_e = 2.5\,\mathrm{km/s}$	$v_e = 3.5\,\mathrm{km/s}$
			Miss distance			
1	0.19711	0.98554	1.97108	2.95662	4.92770	6.89878
2	0.21651	1.08257	2.16514	3.24771	5.41284	7.57798
3	0.16238	0.81188	1.62376	2.43564	4.05940	5.68316
4	0.12990	0.64948	1.29896	1.94845	3.24741	4.54638
5	0.10824	0.54122	1.08245	1.62367	2.70611	3.78856
6	0.09278	0.46390	0.92780	1.39169	2.31949	3.24728
7	0.08118	0.40591	0.81181	1.21772	2.02953	2.84134
8	0.07216	0.36080	0.72160	1.08241	1.80401	2.52561
9	0.06494	0.32472	0.64944	0.97416	1.62359	2.27303
10	0.05904	0.29520	0.59039	0.88559	1.47599	2.06638
15	0.04059	0.20294	0.40589	0.60883	1.01471	1.42060
20	0.03093	0.15462	0.30924	0.46386	0.77311	1.08235
25	0.02498	0.12489	0.24977	0.37466	0.62443	0.87420
30	0.02095	0.10474	0.20949	0.31423	0.52371	0.73320
35	0.01804	0.09019	0.18039	0.27058	0.45097	0.63136
40	0.01584	0.07920	0.15839	0.23758	0.39598	0.55437
45	0.01412	0.07059	0.14117	0.21176	0.35293	0.49411
50	0.01273	0.06367	0.12733	0.19100	0.31833	0.44566

Table 2: Miss distances after a maneuver as a function of power factor and exhaust velocity.

γ	$v_e = 0.1\,\mathrm{km/s}$	$v_e = 0.5\,\mathrm{km/s}$	$v_e = 1.0\,\mathrm{km/s}$	$v_e = 1.5\,\mathrm{km/s}$	$v_e = 2.5\,\mathrm{km/s}$	$v_e = 3.5\,\mathrm{km/s}$
			Miss distance			
10^{-1}	65.07601	325.38004	650.76008	976.14013	1626.90021	2277.66029
10^{-2}	61.70524	308.52620	617.05240	925.57859	1542.63099	2159.68339
10^{-3}	34.70914	173.54569	347.09139	520.63708	867.728480	1214.81986
10^{-4}	5.55706	27.78532	55.57065	83.35597	138.926620	194.49727
10^{-5}	0.58711	2.93555	5.87110	8.80665	14.67776	20.54886
10^{-6}	0.05904	0.29520	0.59039	0.88559	1.47599	2.06638
10^{-7}	0.00591	0.02954	0.05907	0.08861	0.14768	0.20675

propellant mass, and the escape velocity of the gas. The position uncertainty of the spacecraft and the approaching projectile are taken into account, considering also large spacecraft dimensions.

Our results were obtained for initial relative velocities (8.0 km/s) near to LEO mean velocities (10.0 km/s), with time just enough to implement the evasive maneuver. For small spacecrafts and low on-board fuel ($1 < \chi < 10$) in this region would collide with objects of tenth of meters, or even a few kilometers, while mid-size spacecraft ($10 < \chi < 100$) would collide with much smaller objects. Furthermore, we observed that smaller power factors are favorable to collide with smaller objects for any gas ejection velocities, providing collisions with meter size objects ($10^{-7} < \gamma < 10^{-6}$). This means that we can make technological adjustments to the vehicle propulsion system, enabling the spacecraft to avoid the collision with particles with this order. Generally, the results show that the technological parameters are determinant for the set of initial conditions favorable to collisions, in this way, a space

Table 3: Summary of attainable miss distances after a maneuver as a function of initial distance r_0 and exhaust velocity. t_c represents the time taken to reach the closest approach.

r_0	$v_e = 0.1\,\mathrm{km/s}$	$v_e = 0.5\,\mathrm{km/s}$	$v_e = 1.0\,\mathrm{km/s}$	$v_e = 1.5\,\mathrm{km/s}$	$v_e = 2.5\,\mathrm{km/s}$	$v_e = 3.5\,\mathrm{km/s}$	t_c (s)	V_0 (km/s)
				Miss distance				
3.0	0.587110	2.935552	5.871103	8.806655	14.677758	20.548861	2667	7.766403
10.0	0.586520	2.932598	5.865197	8.797795	14.662992	20.528189	2666	7.513203
50.0	0.587701	2.938506	5.877013	8.815519	14.692532	20.569545	2668	7.585059
80.0	0.588293	2.941463	5.882926	8.824388	14.707314	20.590240	2669	7.755845
100.0	0.588884	2.944421	5.888842	8.833263	14.722104	20.610946	2670	7.693744
350.0	0.591254	2.956269	5.912539	8.868808	14.781346	20.693885	2674	7.673087
500.0	0.591256	2.956270	5.912542	8.869875	14.781302	20.693675	2674	8.546885

mission could be controlled from the coefficients of the equation solutions which depends on such parameters, taking into account the relative positions of the collisional objects.

Acknowledgments

The authors wish to thanks CNPq, FAPESP, UEFS, and UNESP for the support and grants received throughout this work.

References

[1] A. Rossi, G. B. Valsecchi, and P. Farinella, "Risk of collisions for constellation satellites," *Nature*, vol. 399, no. 6738, pp. 743–744, 1999.
[2] A. Rossi, G. B. Valsecchi, and P. Farinella, "Collision risk for high inclination satellite constellations," *Planetary and Space Science*, vol. 48, no. 4, pp. 319–330, 2000.
[3] A. Rossi, L. Anselmo, C. Pardini, R. Jehn, and G. B. Valsecchi, "The new space debris mitigation (SDM 4.0) long term evolution code," in *Proceedings of the 5th European Conference on Space Debris*, Darmstadt, Germany, April 2009.
[4] J. C. Liou, "An active debris removal parametric study for LEO environment remediation," *Advances in Space Research*, vol. 47, no. 11, pp. 1865–1876, 2011.
[5] W. H. Clohessy and R. S. Wiltschire, "Terminal guidance system for satellite rendezvous," *Journal of the Aerospace Sciences*, vol. 27, no. 9, pp. 653–659, 1960.
[6] C. D. Murray and S. F. Dermott, *Solar System Dynamics*, Cambridge University Press, 2000.